JCTC Journal of Chemical Theory and Computation

pubs.acs.org/JCTC Article

Nonadiabatic Dynamics in a Laser Field: Using Floquet Fewest Switches Surface Hopping To Calculate Electronic Populations for Slow Nuclear Velocities

Zeyu Zhou, Hsing-Ta Chen, Abraham Nitzan, and Joseph Eli Subotnik*

Cite This: https://dx.doi.org/10.1021/acs.jctc.9b00950 Read Online

ACCESS | Metrics & More | Article Recommendations

ABSTRACT: We investigate two well-known approaches for extending the fewest switches surface hopping (FSSH) algorithm to periodic time-dependent couplings. The first formalism acts as if the instantaneous adiabatic electronic states were standard adiabatic states, which just happen to evolve in time. The second formalism replaces the role of the usual adiabatic states by the time-independent adiabatic Floquet states. For a set of modified Tully model problems, the Floquet FSSH (F-FSSH) formalism gives a better estimate for both transmission and reflection probabilities than the instantaneous adiabatic FSSH (IA-FSSH) formalism, especially for slow nuclear velocities. More importantly, only F-FSSH predicts the correct final scattering momentum. Finally, in order to use Floquet theory accurately, we find that it is crucial to account for the interference between wavepackets on different Floquet states. Our results should be of interest to all those interested in laser-induced molecular dynamics.

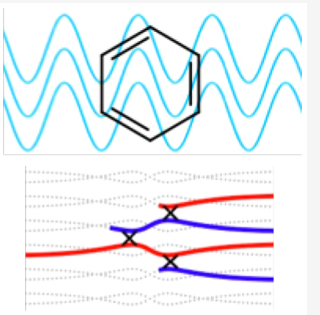

1. INTRODUCTION

Electronic nonadiabatic transitions and photon excitations are among the most important dynamical processes in the field of spectroscopy and photochemistry, and while usually considered separate processes, these phenomena can both enhance or compete with each other. Specifically, electrons in a molecular system interacting with an incident laser field can transition between adiabatic states (i) through the nonadiabatic coupling beyond the Born−Oppenheimer approximation or (ii) through the radiative coupling in conjunction with absorption or emission of photons. Over the past decades, many exciting phenomena, ranging from molecular photodissociation[1−5] to coherent X-ray diffraction,[6,7] have highlighted the importance of the dynamical interplay between nonadiabatic transitions and photoexcitation processes. These recent observations demonstrate a need for accurate theoretical treatments of nonadiabatic molecular dynamics as driven by an external time-dependent field. However, while exact dynamics may be obtained for specific idealized models, most practical simulation schemes for large, realistic systems rely on a mixed quantum−classical framework—treating the electronic degrees of freedom with quantum mechanics and describing the nuclear motions and the laser field using classical mechanics/electrodynamics.

Given the success of semiclassical methodologies for studying nonadiabatic molecular dynamics over the past 30 years, the most natural strategy to capture laser-driven nonadiabatic dynamics is to generalize these semiclassical methods to treat radiative coupling in a similar fashion.[8,9] Today, several different approaches based on Tully's fewest switches surface hopping (FSSH) have been proposed,[10] including the surface hopping including arbitrary couplings (SHARC)[11,12] and field-induced surface hopping (FISH)[13,14] approaches. Each of these approaches applies a modified hopping mechanism to account for the interaction with the laser field. Within these methods, the electronic Hamiltonian is expressed in terms of the classical parameters of the nuclear coordinates and the incident laser field that explicitly depends on time; diagonalizing the electronic Hamiltonian yields the instantaneous adiabatic states and potential energy surfaces (PESs).[15,16] The basic premise of SHARC is to modify Tully's FSSH algorithm with minimal changes to FSSH such that effectively one runs Tully's algorithm on top of an instantaneous adiabatic representation: the electronic wave function evolves according to the Schrödinger equation with the time-dependent Hamiltonian, and a swarm of classical trajectories is propagated along the instantaneous adiabatic PESs. The active PES of each classical trajectory can change from one to another through a hopping event associated with (i) the nuclear-derivative (nonradiative) coupling (which should in theory conserve the total energy of the system) or (ii) the time-derivative (radiative) coupling which allows the electronic system to absorb/emit radiation energy and which does not conserve energy. These so-called instantaneous

Received: September 25, 2019

adiabatic FSSH methods (IA-FSSH) have been used to study gas phase photodissociation[11] and optimal control of the trans−cis isomerization.[17]

Now, despite its growing popularity, IA-FSSH does suffer several drawbacks. First, the FSSH problem of decoherence/recoherence is expected to be exacerbated for driven nonadiabatic dynamics. Since the instantaneous PESs oscillate rapidly at the frequency of the laser field, the electronic coherence becomes more complicated and difficult to recover with FSSH (which does not include any scheme to deal with the repeated separation and recombination of wave packets moving on different PESs[18]). While several decoherence strategies exist,[12,19−36] one might expect fatal problems for driven IA-FSSH nonadiabatic dynamics because recoherence effects cannot be captured by non-interacting FSSH trajectories.[37−40] Second, IA-FSSH treats the absorption/emission of radiation energy as a continuous phenomenon and ignores all quantum features of light. Thus, radiation-induced hopping can occur at any energy difference between two PESs, usually without regard to energy conservation, such that one might expect to find not the most accurate description of energy absorption/emission. One phenomenological means to solve this problem is to allow the radiative hopping only within a restricted bandwidth of the photon energy, but it is unclear how effective this approach will be.

In very recent years, Floquet FSSH (F-FSSH) method has emerged to be an appealing alternative for simulating laser-driven nonadiabatic dynamics, especially for a time-periodic field.[9,41] Unlike the instantaneous adiabatic representation for periodic couplings, F-FSSH eliminates all explicit dependence on time by expanding the electronic wave function in a Floquet state basis (the diabatic states dressed by $e^{im\omega t}$ for an integer m and the laser frequency ω). For a periodic field, the resulting Hamiltonian, the so-called Floquet Hamiltonian, is *time-independent*, albeit of infinite dimension of m. Thus, the Floquet quasi-energy surfaces obtained by diagonalizing the Floquet Hamiltonian are also time-independent, so that one can simply employ the standard FSSH method in the Floquet state representation with a minimal modification: the infinite-dimensional wave function evolves following the Schrödinger equation under the Floquet Hamiltonian, and classical trajectories move along Floquet quasi-energy surfaces. When a classical trajectory passes through a crossing of two Floquet quasi-energy surfaces, the active surface of the classical trajectory can change by Tully's stochastic hopping mechanism while conserving the Floquet quasi-energy. Furthermore, the F-FSSH method can partially account for quantized photon absorption/emission because, by construction, the Floquet quasi-energy surfaces of the same diabatic state are separated by an integer multiple of the photon energy ($m\hbar\omega$).

Nevertheless, despite these positive attributes, in practice, there are several difficulties when implementing the F-FSSH method for driven nonadiabatic dynamics. First, many crossings of Floquet quasi-energy surfaces are trivial crossings; i.e., the derivative coupling becomes infinity at the exact crossing point. For any FSSH simulation carried out with a finite time step, trivial crossings may be missed when propagating a classical trajectory, which leads to unphysical multiphoton excitations. Recently, several approaches have been developed to capture trivial crossings,[42−52] but none have been applied to the F-FSSH method; usually these methods have been applied to simulations with fewer than 20 states, and we will show that some further adjustments are necessary. Second, as we will show below, reconstructing the real electronic wave function from the Floquet wave function requires an accurate treatment of the interference between wavepackets on different Floquet quasi-energy surfaces. When summing over all of the trajectories, the diabatic population includes two contributions: (i) the number of trajectories ending up on the same diabatic state and (ii) the summation over the coherences of the Floquet states associated with each diabatic state. We are unaware of any previous discussion of this point with regard to F-FSSH in the existing literature.

With this background in mind, our goals for this work are to rigorously investigate and compare F-FSSH with IA-FSSH versus the exact solutions for modified versions of two of Tully's model problems. This work is arranged as follows: In section 2, we review both the IA-FSSH and F-FSSH formalisms. In section 3, we summarize the differences and modifications which we have implemented in order to construct meaningful and efficient surface hopping calculations. In section 4, two typical model problems are introduced and the results of both formalisms are compared with exact quantum calculations. We conclude and analyze the advantages and drawbacks of F-FSSH in sections 5 and 6.

Notation. A Floquet basis requires a great number of indices; the notation can be hard to follow. In general, an arrow on the top of a letter denotes a vector. For the reader's convenience, all labels are listed in Table 1.

Table 1. Notation for the Present Paper

variable	definition
$\vec{R}$, $\vec{v}$, M	position, velocity, and mass of nuclei
μ, ν	indices for electronic states
m, n	indices for Fourier expansion
J, K	indices for Floquet states
$\hat{H}_{\text{tot}}$, $\hat{H}_{\text{el}}$	total Hamiltonian and electronic Hamiltonian
$\hat{\mathbb{T}}_{\vec{R}}$	kinetic operator for nuclear DoF
$\lvert\phi_j^{\text{ad}}(\vec{R},t)\rangle$	instantaneous adiabatic basis of the electronic Hamiltonian
c_j	electronic amplitude on instantaneous adiabatic state i
$V_j^{\text{el}}(\vec{R},t)$	eigenvalues of instantaneous electronic Hamiltonian $\hat{H}_{\text{el}}(R,t)$
$\vec{d}_{jk}$	derivative coupling
T_{jk}	time-derivative coupling matrix
$\hat{H}_{\text{F}}$	Floquet Hamiltonian
$\lvert\Phi^J(\vec{R},t)\rangle$	electronic Floquet state J
$\hat{\mathcal{H}}^{\text{F}}$	Floquet Hamiltonian after Fourier transform[a]
$\tilde{c}_J$	electronic amplitude on Floquet state J[b]
ε_J, $\lvert G^J(\vec{R})\rangle$	eigenvalues and eigenvectors of Floquet Hamiltonian $\hat{\mathcal{H}}^{\text{F}}$
$\text{d}t_c$, $\text{d}t_q$	time steps for nuclear and electronic propagation
U_{JK}	overlap matrix with elements $U_{JK}(t_0 + \text{d}t_c/2) = \langle\Phi^J(t_0)\lvert\Phi^K(t_0 + \text{d}t_c)\rangle$

[a]The dimension of this transformed Floquet Hamiltonian is the dimension of the electronic Hamiltonian $\hat{H}_{\text{el}}$ times the number of Fourier modes after truncation. [b]Same dimension as the Floquet Hamiltonian $\hat{\mathcal{H}}^{\text{F}}$.

2. THEORY

2.1. Illustration of the Problem. Consider the case of a molecule illuminated with continuous wave (CW) light. The incoming light acts as a periodic coupling $\hat{V}(t) = \hat{V}(t + T_0)$ between electronic states with period T_0. Thus, the total Hamiltonian has the following form

https://dx.doi.org/10.1021/acs.jctc.9b00950
J. Chem. Theory Comput. XXXX, XXX, XXX−XXX

$$\hat{H}_{\text{tot}}(t) = \hat{\mathbb{T}}_{\vec{R}} + \hat{H}_{\text{el}}^{0} + \hat{V}(t) = \hat{\mathbb{T}}_{\vec{R}} + \hat{H}_{\text{el}}(t) \tag{1}$$

where $\hat{\mathbb{T}}_{\vec{R}}$ is the kinetic operator and $\hat{H}_{\text{el}}^{0}$ is the time-independent electronic Hamiltonian. Any initial wave function can be propagated by the instantaneous propagator

$$|\Psi(t_0 + \mathrm{d}t)\rangle = \exp\left(-\frac{i\hat{H}_{\text{tot}}(t_0)\,\mathrm{d}t}{\hbar}\right)|\Psi(t_0)\rangle \tag{2}$$

For exact calculations in a few dimensions, the propagator can be expanded according to Trötter decomposition

$$\exp\left(-\frac{i\hat{H}_{\text{tot}}(t_0)\,\mathrm{d}t}{\hbar}\right) = \exp\left(-\frac{i\hat{\mathbb{T}}_{\vec{R}}\,\mathrm{d}t}{2\hbar}\right)\exp\left(-\frac{i\hat{H}_{\text{el}}(t_0)\,\mathrm{d}t}{\hbar}\right)\exp\left(-\frac{i\hat{\mathbb{T}}_{\vec{R}}\,\mathrm{d}t}{2\hbar}\right) \tag{3}$$

In practice, the wave function is transformed between the position and momentum representations, for which the electronic Hamiltonian and the kinetic operator are block diagonal or diagonal, respectively. Performing the Fourier transform vastly accelerates full quantum calculations and will allow us to calculate exact results below.[53]

2.2. Instantaneous Adiabatic Fewest Switches Surface Hopping. Fewest switches surface hopping formalism (FSSH) has emerged to be one of the most popular formalisms to describe nonadiabatic processes during the past 30 years. The nuclear degrees of freedom are treated as classical trajectories moving along the adiabatic potential energy surfaces and described by Newton's equation of motion. All nonadiabatic transitions are simulated by hopping process, which depend on the electronic amplitudes (which are propagated according to the time-dependent electronic Schrödinger equation and the nonadiabatic couplings).

As one moves to a time-dependent regime, as proposed by González et al.,[11,12] an intuitive way to extend the formalism is to replace the adiabatic basis $|\phi_j^{\text{ad}}(\vec{R})\rangle$, which parametrically depends on nuclear coordinate $\vec{R}$ in FSSH, by the instantaneous adiabatic electronic basis $|\phi_j^{\text{ad}}(\vec{R}, t)\rangle$, which parametrically depends on both nuclear coordinate $\vec{R}$ and time t.

$$\hat{H}_{\text{el}}(\vec{R}, t)|\phi_j^{\text{ad}}(\vec{R}, t)\rangle = V_j^{\text{el}}(\vec{R}, t)|\phi_j^{\text{ad}}(\vec{R}, t)\rangle \tag{4}$$

If we then expand the electronic wave function in this instantaneous adiabatic electronic basis,

$$|\Psi(\vec{R}, t)\rangle \equiv \sum_j c_j(\vec{R}, t)|\phi_j^{\text{ad}}(\vec{R}, t)\rangle \tag{5}$$

the electronic equation of motion becomes

$$i\hbar\,\frac{\partial c_j(\vec{R}, t)}{\partial t} = H_j^{\text{el}}(\vec{R}, t)\,c_j(\vec{R}, t) - i\hbar\sum_k T_{jk}c_k(\vec{R}, t) \tag{6}$$

Here, T_{jk} is the time-derivative coupling matrix element defined as

$$T_{jk}(t + \mathrm{d}t_c/2) = \left\langle \phi_j^{\text{ad}}(\vec{R}, t)\left|\frac{\mathrm{d}\phi_k^{\text{ad}}(\vec{R}, t + \mathrm{d}t_c)}{\mathrm{d}t}\right.\right\rangle \tag{7}$$

Note that there are two contributions to the time-derivative coupling matrix:

$$\left|\frac{\mathrm{d}\phi_k^{\text{ad}}(\vec{R}, t)}{\mathrm{d}t}\right\rangle = \left|\frac{\partial\phi_k^{\text{ad}}(\vec{R}, t)}{\partial R}\right\rangle\frac{\mathrm{d}\vec{R}}{\mathrm{d}t} + \left|\frac{\partial\phi_k^{\text{ad}}(\vec{R}, t)}{\partial t}\right\rangle \tag{8}$$

Here $\frac{\mathrm{d}\vec{R}}{\mathrm{d}t}$ is the nuclear velocity. The first term arises from the standard change of basis as induced by the nuclear velocity plus the time-independent nonadiabatic coupling. The second term is new and comes directly from the external field that changes in time.

According to refs 11 and 12, because a molecule can absorb energy from light, the IA-FSSH algorithm accepts all hops regardless of any energy restrictions: energy conservation and velocity rescaling are not enforced [in principle, as the authors note, one should require that the energetic transition lie within the bandwidth of the applied EM field]. In practice, we find that by not enforcing energy conservation, the *electronic* populations predicted by IA-FSSH will be most accurate (though see below for the implications vis à vis *nuclear* observables).

2.3. Floquet Theory. Before introducing the F-FSSH formalism, let us briefly review Floquet theory as applied to solving a purely electronic TDSE. For the problem with periodic Hamiltonian $\hat{H}(t) = \hat{H}(t + T_0)$, the time-dependent electronic Schrödinger equation is

$$i\hbar\,\frac{\partial}{\partial t}|\Psi(t)\rangle = \hat{H}(t)|\Psi(t)\rangle \tag{9}$$

and the initial wave function is

$$|\Psi(t = 0)\rangle = \sum_\mu c_\mu(t = 0)|\mu\rangle \tag{10}$$

Here, $|\mu\rangle$ is a complete, time-independent basis.

Floquet theory expands the solution to eq 9 in the following form

$$|\Psi(t)\rangle = \sum_{m\mu}\tilde{c}_{m\mu}(t)\exp(im\omega t)|\mu\rangle \tag{11}$$

or, for short,

$$|\Psi(t)\rangle = \sum_{m\mu}\tilde{c}_{m\mu}(t)|\Xi^{m\mu}(t)\rangle \tag{12}$$

where

$$|\Xi^{m\mu}(t)\rangle \equiv \exp(im\omega t)|\mu\rangle \tag{13}$$

Here, $|\Xi^{m\mu}(t)\rangle$ is the Floquet basis, $\{|\mu\rangle\}$ is a set of electronic basis functions, and m formally runs from $-\infty$ to ∞ (though, in practice, a cutoff is applied). If we plug eq 11 into the TDSE (eq 9), we find

https://dx.doi.org/10.1021/acs.jctc.9b00950
J. Chem. Theory Comput. XXXX, XXX, XXX−XXX

$$\sum_{m\mu} i\hbar \frac{\partial \tilde{c}_{m\mu}(t)}{\partial t}|\Xi^{m\mu}(t)\rangle + \sum_{m\mu} \tilde{c}_{m\mu}(t) i\hbar \frac{\partial}{\partial t}|\Xi^{m\mu}(t)\rangle = \sum_{m\mu} \tilde{c}_{m\mu}(t)\hat{H}(t)|\Xi^{m\mu}(t)\rangle$$

$$\sum_{m\mu} i\hbar \frac{\partial \tilde{c}_{m\mu}(t)}{\partial t}|\Xi^{m\mu}(t)\rangle = \sum_{m\mu} \tilde{c}_{m\mu}(t)\left(\hat{H}(t) - i\hbar \frac{\partial}{\partial t}\right)|\Xi^{m\mu}(t)\rangle \tag{14}$$

We define the Floquet Hamiltonian as

$$\hat{H}_F(t) \equiv \hat{H}(t) - i\hbar \frac{\partial}{\partial t} \tag{15}$$

so that eq 15 becomes

$$\sum_{m\mu} i\hbar \frac{\partial \tilde{c}_{m\mu}(t)}{\partial t} \exp(im\omega t)|\mu\rangle = \sum_{m\mu} \tilde{c}_{m\mu}(t)\hat{H}_F(t) \exp(im\omega t)|\mu\rangle \tag{16}$$

At this point, we use the fact that $\hat{H}(t)$ is periodic in time so that we can expand an arbitrary matrix element of $\hat{H}_F(t)$ as a Fourier sum

$$\langle \nu|\hat{H}_F(t)|\Xi^{m\mu}\rangle = \sum_n \hat{\mathcal{H}}^F_{(n\nu)(m\mu)} \exp[in\omega t] \tag{17}$$

$\hat{\mathcal{H}}^F_{(n\nu)(m\mu)}$ is the Fourier transform of the Floquet Hamitonian $\hat{H}_F$, which can be easily computed as:

$$[\hat{\mathcal{H}}^F]_{(n\nu)(m\mu)} = \frac{1}{T_0}\int_0^{T_0} dt \langle \nu|\hat{H}_F|\Xi^{m\mu}\rangle \exp[-in\omega t] = \frac{1}{T_0}\int_0^{T_0} dt \langle \nu|\hat{H}(t)|\mu\rangle \exp[-i(n-m)\omega t] + \delta_{\mu\nu}\delta_{mn} n\hbar\omega \tag{18}$$

where we have used the identity eq 13. Note that $\hat{\mathcal{H}}^F$ is Hermitian because $\hat{H}(t)$ is Hermitian. Now if we multiply both sides of eq 14 by $\langle \nu|$ and gather all terms proportional to $\exp(in\omega t)$, we find

$$i\hbar \frac{\partial \tilde{c}_{n\nu}(t)}{\partial t} = \sum_{m\mu} \tilde{c}_{m\mu}(t)\hat{\mathcal{H}}^F_{(n\nu)(m\mu)} \tag{19}$$

Equation 19 can clearly be solved with the exponential operator because the entire $\hat{\mathcal{H}}^F$ is time-independent.

$$\tilde{c}_{n\nu} = \sum_{m\mu} [e^{-i\hat{\mathcal{H}}^F t/\hbar}]_{(n\nu)(m\mu)} \tilde{c}_{m\mu} \tag{20}$$

In this sense, it is natural to focus on the eigenstates $|G^J\rangle$ of the Fourier transform of the Floquet Hamiltonian, defined by

$$\hat{\mathcal{H}}^F|G^J\rangle = \varepsilon_J|G^J\rangle \tag{21}$$

Clearly, in a Floquet eigenbasis, propagating the TDSE is simple. Let

$$|\Phi^J(t)\rangle = \sum_{m\mu} G^J_{m\mu} \exp(im\omega t)|\mu\rangle \tag{22}$$

so that

$$\hat{H}_F|\Phi^J(t)\rangle = \sum_{m\mu}\left(\sum_{n\nu} \hat{\mathcal{H}}^F{}_{(m\mu)(n\nu)} G^J_{n\nu}\right)\exp(im\omega t)|\mu\rangle = \varepsilon_J \sum_{m\mu} G^J_{m\mu} \exp(im\omega t)|\mu\rangle = \varepsilon_J|\Phi^J(t)\rangle \tag{23}$$

Then if we expand:

$$|\Psi(t)\rangle \equiv \sum_J \tilde{c}_J(t)|\Phi^J(t)\rangle \tag{24}$$

eq 9 becomes

$$\sum_J i\hbar \frac{\partial \tilde{c}_J(t)}{\partial t}|\Phi^J(t)\rangle = \sum_J \tilde{c}_J(t)\varepsilon_J|\Phi^J(t)\rangle \tag{25}$$

whose solution is simply

$$\tilde{c}_J(t) = \tilde{c}_J(t=0) \exp(-i\varepsilon_J t/\hbar) \tag{26}$$

Solving eq 21 is a simple mean of propagating the TDESE in a periodic field.

2.4. Wavepacket Dynamics with Floquet States. Now, let us review how Floquet theory is applied to wavepacket dynamics with nuclear motion involved. The TDSE for the total nuclear−electronic wave function with nuclear coordinate $\vec{R}$ is

$$i\hbar \frac{\partial}{\partial t}|\Psi(t)\rangle = \hat{H}_{tot}(t)|\Psi(t)\rangle = \hat{\mathbb{T}}_R + \hat{H}_{el}(t)|\Psi(t)\rangle \tag{27}$$

The initial electronic wave function at nuclear position $\vec{R}$ is

$$\langle \vec{R}|\Psi(t=0)\rangle = \sum_\mu c_\mu(\vec{R}, t=0)|\mu\rangle \tag{28}$$

According to Floquet theory, we express the electronic wave function in eq 27 in the following form:

$$\langle \vec{R}|\Psi(t)\rangle = \sum_J \tilde{c}_J(\vec{R}, t)|\Phi^J(\vec{R}, t)\rangle \tag{29}$$

where for now J can be any electronic basis.

By plugging eq 29 into the TDSE (eq 27), we obtain

$$i\hbar \sum_J \frac{\partial \tilde{c}_J(\vec{R}, t)}{\partial t}|\Phi^J(\vec{R}, t)\rangle + i\hbar \sum_J \tilde{c}_J(\vec{R}, t) \frac{\partial|\Phi^J(\vec{R}, t)\rangle}{\partial t} = (\hat{\mathbb{T}}_{\vec{R}} + \hat{H}_{el})|\Psi(\vec{R}, t)\rangle$$

$$\Rightarrow i\hbar \sum_J \frac{\partial \tilde{c}_J(\vec{R}, t)}{\partial t}|\Phi^J(\vec{R}, t)\rangle = \hat{\mathbb{T}}_{\vec{R}}\left(\sum_J \tilde{c}_J(\vec{R}, t)|\Phi^J(\vec{R}, t)\rangle\right) + \sum_J \tilde{c}_J(\vec{R}, t)\hat{H}^{el}_F(t)|\Phi^J(\vec{R}, t)\rangle \tag{30}$$

Again, we have defined the electronic Floquet Hamiltonian as

$$\hat{H}^{el}_F(t) \equiv \hat{H}_{el}(t) - i\hbar \frac{\partial}{\partial t} \tag{31}$$

https://dx.doi.org/10.1021/acs.jctc.9b00950
J. Chem. Theory Comput. XXXX, XXX, XXX−XXX

The nuclear TDSE in eq 30 can be solved either in a diabatic electronic basis (where $J = (m\mu)$) or an adiabatic basis (where J labels an adiabatic Floquet state).

2.4.1. Wavepacket Dynamics in a Diabatic Floquet Representation. Assuming a diabatic representation,

$$|\Phi^J(t)\rangle \equiv |\Xi^{m\mu}(t)\rangle = \exp(im\omega t)|\mu\rangle \tag{32}$$

we can solve the TDSE in eq 30 by expanding the Floquet Hamiltonian (eq 31) as a function of time as in eq 17 and comparing only terms with the same Fourier mode $\exp(in\omega t)$ and electronic state $|\nu\rangle$. We will obtain an equation similar to eq 19

$$i\hbar \frac{\partial \tilde{c}_{n\nu}(\vec{R}, t)}{\partial t} = \hat{\mathbb{T}}_{\vec{R}} \tilde{c}_{n\nu}(\vec{R}, t) + \sum_{m\mu} \hat{\mathcal{H}}^{\mathrm{F}}_{(n\nu)(m\mu)} \tilde{c}_{m\mu}(\vec{R}, t) \tag{33}$$

Equation 33 is effectively a time-independent Schrödinger equation and can be easily solved.

2.4.2. Wavepacket Dynamics under Adiabatic Floquet Representation. Assuming an adiabatic representation, the relevant Floquet basis is

$$|\Phi^J(\vec{R}, t)\rangle = \sum_{\mu m} G^J_{m\mu}(\vec{R}) \exp(im\omega t)|\mu\rangle \tag{34}$$

By plugging the adiabatic Floquet basis into eq 30 and using the fact that the eigenvalues of $\hat{H}_{\mathrm{F}}(t)$ are time-independent (for a periodic electronic Hamiltonian, see eq 23)

$$\hat{H}^{\mathrm{el}}_{\mathrm{F}} |\Phi^J(\vec{R}, t)\rangle = \varepsilon(\vec{R})|\Phi^J(\vec{R}, t)\rangle \tag{35}$$

we find

$$\begin{aligned} & i\hbar \sum_J \frac{\partial \tilde{c}_J(\vec{R}, t)}{\partial t}|\Phi^J(\vec{R}, t)\rangle \\ & = \sum_J \varepsilon_J \tilde{c}_J(\vec{R}, t)|\Phi^J(\vec{R}, t)\rangle + \hat{\mathbb{T}}_{\vec{R}}\Big(\sum_J \tilde{c}_J(\vec{R}, t)|\Phi^J(\vec{R}, t)\rangle\Big) \end{aligned} \tag{36}$$

If we apply $\langle\nu|\otimes$ and compare only those terms with the same Fourier mode, $\exp(in\omega t)$, we find

$$\begin{aligned} & \sum_J i\hbar \frac{\partial \tilde{c}_J(\vec{R}, t)}{\partial t} G^J_{n\nu}(\vec{R}) \\ & = \sum_J \varepsilon_J \tilde{c}_J(\vec{R}, t) G^J_{n\nu}(\vec{R}) + \sum_J \hat{\mathbb{T}}_{\vec{R}}(\tilde{c}_J(\vec{R}, t) G^J_{n\nu}(\vec{R})) \\ & = \sum_J \varepsilon_J \tilde{c}_J(\vec{R}, t) G^J_{n\nu}(\vec{R}) - \sum_J \frac{\hbar^2}{2M}(\nabla_{\vec{R}}{}^2 \tilde{c}_J(\vec{R}, t)) G^J_{n\nu}(\vec{R}) \\ & \quad - \sum_J \frac{\hbar^2}{M}(\nabla_{\vec{R}} \tilde{c}_J(\vec{R}, t))(\nabla_{\vec{R}} G^J_{n\nu}(\vec{R})) \\ & \quad - \sum_J \frac{\hbar^2}{2M} \tilde{c}_J(\vec{R}, t)(\nabla_{\vec{R}}{}^2 G^J_{n\nu}(\vec{R})) \end{aligned} \tag{37}$$

After applying $\sum_{n\nu} G^{K*}_{n\nu}\otimes$ on both sides and using the fact that

$$\sum_{n\nu} G^{K*}_{n\nu} G^J_{n\nu} = \delta_{JK} \tag{38}$$

we obtain

$$\begin{aligned} i\hbar \frac{\partial \tilde{c}_K(\vec{R}, t)}{\partial t} &= \varepsilon_K(\vec{R}) \tilde{c}_K(\vec{R}, t) - \frac{\hbar^2}{2M} \nabla_{\vec{R}}{}^2 \tilde{c}_K(\vec{R}, t) \\ & \quad - \frac{\hbar^2}{M} \sum_J \nabla_{\vec{R}} \tilde{c}_J(\vec{R}, t) \langle G^K(\vec{R})|\nabla_{\vec{R}} G^J(\vec{R})\rangle \\ & \quad - \frac{\hbar^2}{2M} \sum_J \tilde{c}_J(\vec{R}, t) \langle G^K(\vec{R})|\nabla_{\vec{R}}{}^2 G^J(\vec{R})\rangle \end{aligned} \tag{39}$$

Again, eq 39 appears to be entirely time-independent and can be easily solved. Note that the probability to measure electronic state $|\nu\rangle$ is

$$\begin{aligned} |\langle\nu|\Psi(t)\rangle|^2 &= \int \mathrm{d}\vec{R} \left| \sum_J \tilde{c}_J(\vec{R}, t) \sum_m G^J_{m\nu}(\vec{R}) \exp(im\omega t) \right|^2 \\ &= \int \mathrm{d}\vec{R} \sum_J \left| \tilde{c}_J(\vec{R}, t) \sum_m G^J_{m\nu} \right|^2 \\ & \quad + \int \mathrm{d}\vec{R} \sum_{J,K} \tilde{c}_J(\vec{R}, t) \tilde{c}^*_K(\vec{R}, t) \\ & \quad \times \sum_{m\neq n} G^J_{n\nu}(\vec{R})(G^K_{m\nu}(\vec{R}))^* \exp[i(n-m)\omega t] \end{aligned} \tag{40}$$

In eq 40, we find two terms that must be added together to find the total probability on electronic state $|\nu\rangle$.

In the limit of no coupling (when adiabats and diabats are identical), $G^J_{m\nu} = \delta_{J,(m\nu)}$, and

$$\begin{aligned} |\langle\nu|\Psi(t)\rangle|^2 &= \int \mathrm{d}\vec{R} \sum_m |\tilde{c}_{m\nu}(\vec{R}, t)|^2 \\ & \quad + \int \mathrm{d}\vec{R} \sum_{m\neq n} \tilde{c}_{n\nu}(\vec{R}, t) \tilde{c}^*_{m\nu}(\vec{R}, t) \exp[i(n-m)\omega t] \end{aligned} \tag{41}$$

2.5. F-FSSH Algorithm. At last, we can present the F-FSSH algorithm. In general, surface hopping is valid only in an adiabatic representation.[54,57,58] The nuclear motion in F-FSSH is described by Newton's equations of motion

$$\begin{aligned} \dot{\vec{R}} &= \vec{v} \\ \dot{\vec{v}} &= -\frac{\nabla_{\vec{R}} \varepsilon_J(\vec{R})}{M} \end{aligned}$$

where $\varepsilon_J(\vec{R})$ is the adiabatic quasi-energy of the active Floquet state J; see eq 35. After dropping the second derivative coupling term in eq 39, the corresponding equations of motion for the electronic degrees of freedom are

$$\begin{aligned} i\hbar \frac{\partial \tilde{c}_J(\vec{R}, t)}{\partial t} &= \varepsilon_J(\vec{R}) \tilde{c}_J(\vec{R}, t) - i\hbar \sum_K \vec{v} \cdot \vec{d}_{JK} \tilde{c}_K(\vec{R}, t) \\ &= \varepsilon_J(\vec{R}) \tilde{c}_J(\vec{R}, t) - i\hbar \sum_K T_{JK} \tilde{c}_K(\vec{R}, t) \end{aligned} \tag{42}$$

Here, $\vec{d}_{JK}$ is the derivative coupling $\langle G^K(\vec{R})|\nabla_{\vec{R}} G^J(\vec{R})\rangle$ between Floquet states J and K. T is the time-derivative coupling matrix (see eq 7). According to F-FSSH, the hopping probability from active Floquet state J to state K is

https://dx.doi.org/10.1021/acs.jctc.9b00950
J. Chem. Theory Comput. XXXX, XXX, XXX−XXX

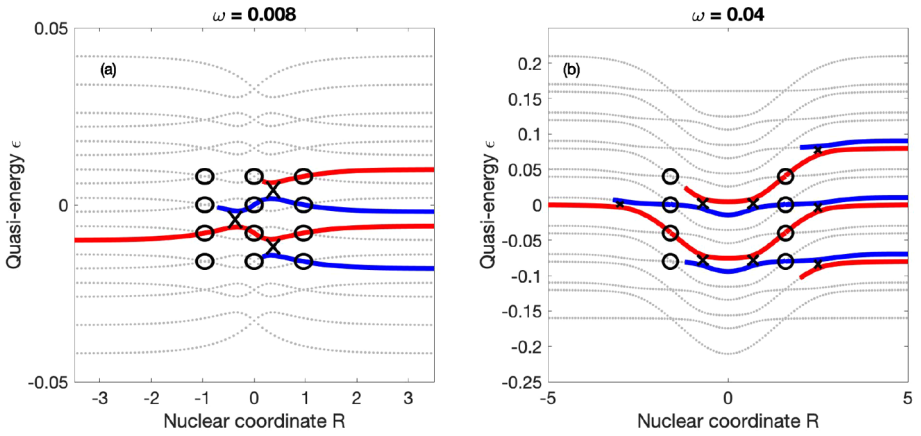

Figure 1. Floquet states and possible transmission Floquet channels for (a) the modified simple avoided crossing problem with $\omega = 0.008$ and (b) the modified dual avoided crossing problem with $\omega = 0.040$ (see eqs 47 and 48). Both figures are truncated at $m = \pm 4$. The solid circles highlight trivial crossings, and the solid arrows highlight real avoided crossings. The trajectories start from the left on the red state (diabat $|0\rangle$) and moving to the right. As particles move along the Floquet potential quasi-energy surface, trajectories may or may not hop between these Floquet states near avoided crossings and must hop at trivial crossings in order to remain on the same diabatic state.

$$g_{JK} = \frac{-2\mathrm{Re}(\tilde{c}_J \tilde{c}_K^* T_{KJ})}{|\tilde{c}_J|^2}\,\mathrm{d}t \tag{43}$$

If g_{JK} is less than 0 for any K, we set $g_{JK} = 0$.

After each successful hop, the velocity is adjusted to conserve the total Floquet quasi-energy. Unlike IA-FSSH, frustrated hops are not allowed.

2.6. Nuances of the F-FSSH Algorithm. For exact wavepacket calculations in a Floquet basis, the exact total probability on a given electronic state ν is calculated by the coherent sum in eq 41. Thus, for surface hopping to match exact wavepacket dynamics, we must evaluate both the diagonal and interference terms in eq 41. The diagonal contribution is simple:

$$\mathrm{Prob}_\nu^{\mathrm{pop}} = \frac{\sum_m N_{m\nu}^{\mathrm{traj}}}{N_{\mathrm{tot}}} \tag{44}$$

Here, N_{tot} is the number of all independent trajectories, and $N_{m\nu}^{\mathrm{traj}}$ is the number of the trajectories ending up asymptotically on a Floquet state with indices $m\nu$. In other words, if the active surface is labeled J,

$$N_{\mathrm{m}\nu}^{\mathrm{traj}} = \sum_{r=1}^{N_{\mathrm{tot}}} \delta_{J,(\mathrm{m}\nu)}^r \tag{45}$$

where we index trajectories by r.

For the interference term, we will make the following approximation:

$$\mathrm{Prob}_\nu^{\mathrm{interference}} = \sum_{n\neq m} \frac{\sum_{r=1}^{N_{n\nu}^{\mathrm{traj}}} \sum_{s=1}^{N_{m\nu}^{\mathrm{traj}}} \tilde{c}_{n\nu}^r (\tilde{c}_{m\nu}^s)^* \exp(i(n-m)\omega t)}{N_{n\nu}^{\mathrm{traj}} \times N_{m\nu}^{\mathrm{traj}}} \tag{46}$$

Here, $\tilde{c}_{\mathrm{n}\nu}^r$ is the electronic amplitutde on Floquet state $(n\nu)$ at the end of the rth trajecrory. In eq 46, we have attempted to calculate the interference term in eq 41 by using the electronic amplitude $(\tilde{c}_J(t))$ to give us phase information about wavepackets propagating on state J, in keeping with the density matrix interpretation of FSSH as given in ref 35 (see section III in ref 35, which relates it to the QCLE[55−58]). All of the independent trajectories are propagated for a certain amount of time t, which is long enough for all trajectories to pass through the interaction zone.

3. SIMULATION DETAILS

In this work, for simplicity, we will focus on one-dimensional models and specifically time-periodic variants of the famous Tully model problems.[10]

3.1. Model Problems. Tully's simple avoided crossing model problem is modified in the diabatic representation as

$$\begin{aligned} H_{00}^{\mathrm{el}}(R) &= A[1 - \exp(-BR)], \quad R > 0 \\ H_{00}^{\mathrm{el}}(R) &= -A[1 - \exp(BR)], \quad R < 0 \\ H_{11}^{\mathrm{el}}(R) &= -H_{00}^{\mathrm{el}}(R) \\ H_{01}^{\mathrm{el}}(R, t) &= H_{10}^{el}(R, t) = C \exp(-DR^2) \cos \omega t \\ &= V(R) \cos \omega t \end{aligned} \tag{47}$$

The parameters are the same as those in the original work, $A = 0.01$, $B = 1.6$, $C = 0.005$, and $D = 1.0$, and we will test two different ω cases, $\omega = 0.008$ and 0.012.

Tully's dual avoided crossing model problem is modified in a similar fashion

$$\begin{aligned} H_{00}^{\mathrm{el}}(R) &= 0 \\ H_{11}^{\mathrm{el}}(R) &= -A \exp(-BR^2) + E_0 \\ H_{01}^{\mathrm{el}}(R, t) &= H_{10}^{\mathrm{el}}(R, t) \\ &= C \exp(-DR^2) \cos \omega t \\ &= V(R) \cos \omega t \end{aligned} \tag{48}$$

The parameters are $A = 0.10$, $B = 0.28$, $E_0 = 0.05$, $C = 0.015$, $D = 0.06$, and $\omega = 0.02$,0.04.

As discussed in sections 1 and 2.2, IA-FSSH propagates trajectories along the instantaneous PESs. To better understand IA-FSSH, note that according to eqs 47 and 48, in our model problems, the number of avoided crossings remains the same and they remain at the same position, but the strength of the instantaneous diabatic coupling oscillates.

Unlike IA-FSSH, however, Floquet theory is more complicated. The potential quasi-energy surfaces generated are worth further discussion. The Floquet Hamiltonian $\hat{\mathcal{H}}_{\mathrm{F}}^{\mathrm{el}}$ after Fourier transform is shown below.

https://dx.doi.org/10.1021/acs.jctc.9b00950
J. Chem. Theory Comput. XXXX, XXX, XXX−XXX

$$\hat{\mathcal{H}}_F^{el}(R) = \begin{bmatrix} \ddots & & & & \\ & H_{00}^{el}(R)+\hbar\omega & V(R)/2 & & \\ & & H_{11}^{el}(R)+\hbar\omega & V(R)/2 & \\ & V(R)/2 & & H_{00}^{el}(R) & V(R)/2 \\ & V(R)/2 & & H_{11}^{el}(R) & V(R)/2 \\ & & V(R)/2 & & H_{00}^{el}(R)-\hbar\omega \\ & & V(R)/2 & & H_{11}^{el}(R)-\hbar\omega \\ & & & & \ddots \end{bmatrix}$$

Here, $V(R)$ is the time-independent part of the coupling $H_{01}^{el}(R, t)$ and $H_{10}^{el}(R, t)$. The adiabatic potential quasi-energy surfaces are obtained by diagonalizing the electronic Floquet Hamiltonian $\hat{\mathcal{H}}_F^{el}$. As shown in Figure 1, relative to the original time-independent Tully models, F-FSSH can include many more than one avoided crossing, and light-induced trivial crossings (black circles) and avoided crossings (black crosses) are both possible. In particular, note that the original crossings in the time-independent models become a set of trivial crossings in Figure 1.

3.2. Exact Calculation. As a benchmark for our semiclassical calculations, we will perform exact dynamic simulations. A Gaussian wavepacket is initialized on diabat $|0\rangle$

$$|\Psi(R, t=0)\rangle = \sqrt[4]{\frac{1}{\pi\sigma^2}} \exp\left(-\frac{(R-R_0)^2}{2\sigma^2} + \frac{iP_0(R-R_0)}{\hbar}\right)|0\rangle \tag{49}$$

Here, R_0 and P_0 are the initial position and momentum, and σ is the width of the Gaussian which is chosen to be $\sigma = 20\hbar/P_0$. The wavepacket is propagated by the propagator in eq 3 with the full, instantaneous Hamiltonian.

3.3. Initial Conditions. For the exact, IA-FSSH, and F-FSSH calculations, we choose $R_0 = -9.0$ which is far enough from $R = 0$ such that there is never any coupling at the initial time. The initial coordinates and momenta of all trajectories for both the IA-FSSH and F-FSSH calculations are sampled from the Wigner distribution of the Gaussian wavepacket:

$$W(R, P) = \frac{1}{\hbar}\exp\left(-\frac{(R-R_0)^2}{\sigma^2}\right)\exp\left(-\frac{(P-P_0)^2\sigma^2}{\hbar^2}\right)$$

For F-FSSH, Floquet theory generates a set of Floquet states with different Fourier modes from a single electronic state. Note that to the left of the coupling regime, the diabatic and adiabatic electronic states are identical. The independent trajectories are initialized on the Floquet state generated by the diabat $|0\rangle$ with Fourier index 0; i.e., the Floquet quasi-energy is the same as the energy of the diabat $|0\rangle$ at R_0.

3.4. Truncation of *m*. In principle, the Fourier series in eq 17 should sum from $-\infty$ to ∞; i.e., the Floquet Hamiltonian $\hat{\mathcal{H}}_F$ should be infinitely large, which would be impossible to diagonalize. However, as a practical matter, we can truncate highly oscillating states. In this work, for the Hamiltonian in eqs 47 and 48, all off-diagonal Hamiltonian matrix elements are of the form $V(R)\cos(\omega t)$, such that only $m = \pm 1$ changes are possible. To calculate the quasi-energies accurately, we find that truncation at $m = \pm 4$ is usually converged (unless otherwise noted).

3.5. Separation of Time Scale between Classical and Quantum Degrees of Freedom. For both F-FSSH and IA-FSSH, nuclear motion is propagated with classical time-step dt_c and the electronic wave function is propagated with a smaller quantum time-step dt_q, which is determined by[50]

$$dt_q' = \min\begin{pmatrix} dt_c \\ 0.02/\max[\epsilon_K - \bar{\epsilon}] \\ 0.02/\max[T] \end{pmatrix}$$

$$dt_q = \frac{dt_c}{\mathrm{nint}(dt_c/dt_q')} \tag{50}$$

Here, $\max[T]$ represents the greatest element in the time-derivative coupling matrix, $\bar{\epsilon}$ is the average of all quasi-energies $\{\epsilon_K\}$, and $\mathrm{nint}(x)$ is the smallest integer that is greater than x. We check for a hop at every dt_q time step, but there should be at most one successful hop within a single dt_c.

3.6. Evaluating the Derivative Coupling d_{JK}. When two diabatic states of a molecule cross with each other, two scenarios are possible. First, the crossing can be meaningful with a finite diabatic coupling, leading to a finite probability of switching diabats. Second, when there is effectively no coupling between surfaces, the molecule must always remain on the same diabat as it leaves the crossing point. The nonadiabatic coupling is either undefined or, with machine error, approaches infinity. This second type of crossing has been called a trivial crossing,[42−52] and often leads to numerical instabilities (requiring very small time steps). Trivial crossings are common in F-FSSH; see the circles in Figure 1.

In order to alleviate the problem of trivial crossings, an overlap matrix scheme has been proposed in refs 49 and 50. The basic idea is to calculate the time-averaged derivative coupling matrix by first calculating the overlap matrix U_{JK} at different times and second evaluating the time-derivative coupling matrix T_{JK}, which is the logarithm of U_{JK}.

$$v\cdot d_{JK} = T_{JK} = \frac{1}{dt_c}\log[U_{JK}]$$

$$U_{JK} = \langle\Phi^J(R(t))|\Phi^K(R(t+dt_c))\rangle \tag{51}$$

The matrix logarithm can be stably realized by a Schur decomposition.[59] Of course, for the logarithm to be real, the signs of eigenvectors $|\Phi_J(R)\rangle$ must be adjusted to guarantee that the overlap matrix U_{JK} is a rotation matrix.

Unfortunately, one shortcoming of the overlap approach just mentioned is the fact that choosing the signs of each adiabatic state can be nontrivial. Thus, for example, all sign combinations are possible for U:

$$MU = \begin{bmatrix} \pm 1 & & & \\ & \pm 1 & & \\ & & \ddots & \\ & & & \pm 1 \end{bmatrix} U$$

Here, M is an arbitrary diagonal matrix with ± 1 along the diagonal, and there are 2^N possible matrices for U, where N is the size of the matrix U. With this problem in mind, in a companion paper,[60] we show that choosing the sign of U to minimize $\|\log(MU)\|$ is a stable, practical, and accurate ansatz. We believe this should definitively solve the trivial crossing sign problem, and we will have further discussion on the more general form of this algorithm in the following work in this issue.[60]

https://dx.doi.org/10.1021/acs.jctc.9b00950
J. Chem. Theory Comput. XXXX, XXX, XXX−XXX

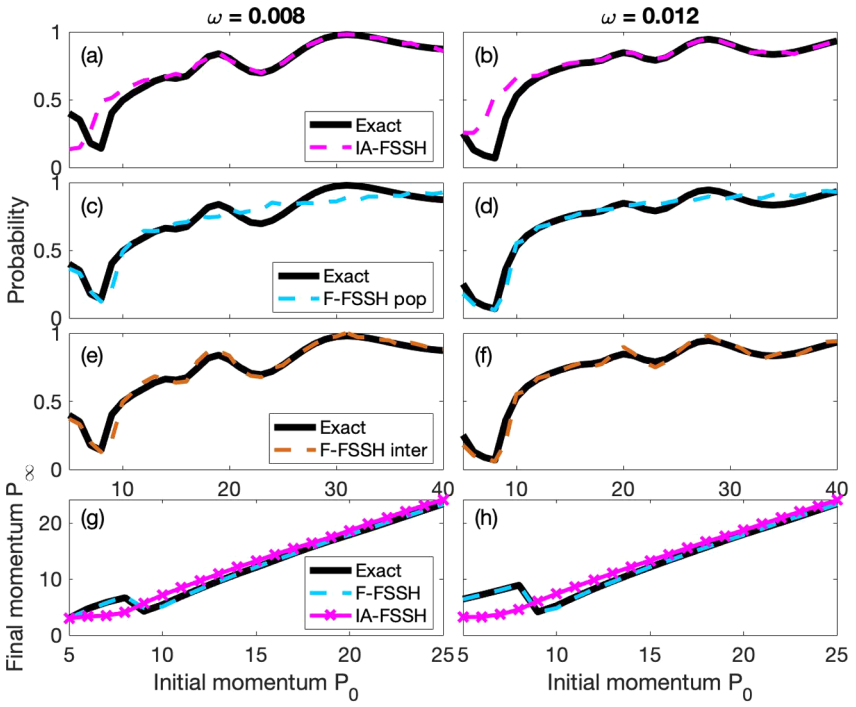

Figure 2. Transmission probabilities and the final momentum on diabat $|0\rangle$ for the modified simple avoided crossing problem with initial state on diabat $|0\rangle$ at $R = -9$. Panels a, c, e, and g on the left represent results with $\omega = 0.008$, and the four panels b, d, f, and h on the right side represent results with $\omega = 0.012$. Panels a and b are plots of the transmission probability on diabat $|0\rangle$ transmission channel for surface hopping with instantaneous adiabatic states (IA-FSSH) versus that of exact dynamics. The results clearly show that IA-FSSH can recover the correct results only in the high kinetic energy regime. Panels c and d are plots of F-FSSH results according to eq 44, while panels e and f are plots of the exact results versus F-FSSH results as estimated by eq 46. Clearly, the interference term is needed at high momentum and including this term makes F-FSSH much more accurate. Panels g and h are plots of the final momenta on diabat $|0\rangle$ transmission channel after passing through the interaction zone. The kinks in the low momentum regime arise from opening up a new channel in Floquet space (see Figure 1), and the fact that both exact and F-FSSH results predict such a kink is strong evidence that energy absorption/emission is treated properly with F-FSSH.

3.7. Velocity Reversal. Implementing velocity reversal after a frustrated hop is known to be crucial when calculating nonadiabatic rates (e.g., Marcus theory[61]). Velocity reversal improves the branching ratios in the surface hopping algorithm.[62] For the one-dimensional model problems below, we will reverse velocity if a frustrated hop between active state λ and target state η occurs and if $v \cdot F_\eta < 0$ and $F_\eta \cdot F_\lambda < 0$.

3.8. Obtaining the Electronic Amplitudes and Momenta for Calculating the Interference Terms in Equation 46. For the scattering calculations below, we will record the electronic amplitude of the active Floquet state and the instantaneous momentum in memory at the end of each trajectory. Afterward, one must calculate the average interference term according to eq 46. A few nuances should now be explained.

First, for FSSH, the signs of the electronic amplitudes are always defined by using the overlap matrix scheme in section 3.6. However, in principle, each trajectory can choose its own sign for the adiabatic electronic states. Thus, in order to calculate the interference term in eq 46, we must be sure that the electronic states (at the end of each dynamical trajectory) all have a consistent definition.[51] For that purpose, we must record the sign changes along each trajectory, multiply all overlap matrices, and obtain the total overlap matrix U^{tot} from the beginning to end:

$$U^{\text{tot}} = \prod_{t=0}^{\infty} U(t) \tag{52}$$

For simplicity, we will initialize all calculations with adiabats equal to diabats and we will insist that, asymptotically (at the end of the trajectory), the adiabats are still equal to the diabats. Thus, if $U^{\text{tot}}_{jk} = -1$ (for each column k, there will only be one non-zero element $U^{\text{tot}}_{jk} = \pm 1$), we will change the sign of $\tilde{c}_k$ at the end of the trajectory.

Second, asymptotically, far away from the crossings, each Floquet state corresponds to a single diabatic electronic state $|\nu\rangle$, so when evaluating eq 46, for the probability to occupy diabatic state $|\nu\rangle$, we sum over only those trajectories ending with an active Floquet state corresponding to electronic state $|\nu\rangle$.

Third, for the two electronic amplitudes ($\tilde{c}^r_{n\nu}$ and $\tilde{c}^s_{m\nu}$) in eq 46, note that these sets correspond to trajectories ending on states with different Fourier indices m and n but the same ν: we average over all combinations of trajectories ending on different $m\nu$ and $n\nu$. We never average amplitudes over different trajectories ending up on the same $(m\nu)$ state: for these matrix elements, we use only the active surface to estimate populations in a fashion consistent with the density matrix interpretation of surface hopping trajectories (method #3 in ref 35).

3.9. Normalization. If we sum the probabilties to occupy all diabatic states j, we should ideally recover unity. However, in practice, when we use F-FSSH, we find a problem. On the one hand, the diagonal contribution in eq 44 is 1. On the other hand, the contributions from the interference terms in eq 46 may not be equal and opposite with each other, which results in incomplete cancellation; i.e., $\sum_\nu \text{Prob}^{\text{interference}}_\nu \neq 0$. Beyond

https://dx.doi.org/10.1021/acs.jctc.9b00950
J. Chem. Theory Comput. XXXX, XXX, XXX−XXX

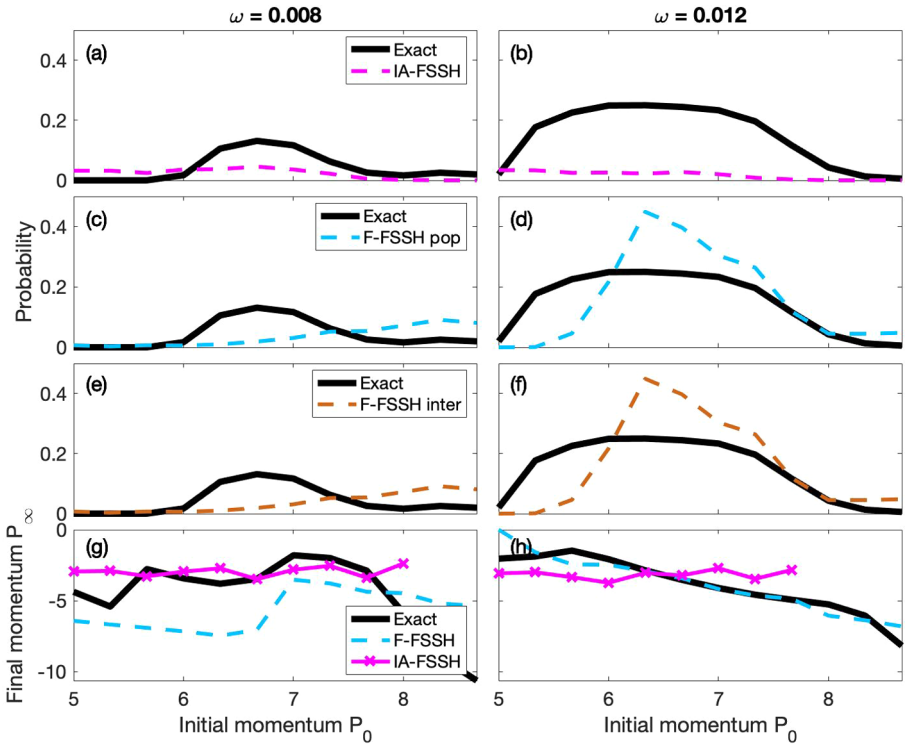

Figure 3. Reflection probabilities and the final momentum on the diabat $|1\rangle$ for the modified simple avoided crossing problem. All figures represent the same physical quantities as in Figure 2 except now we plot the reflection channel. Reflection onto diabat $|1\rangle$ does not occur for the time-independent simple avoided crossing problem, i.e., in the absence of an external time-dependent field.

fixing up this coherence problem with F-FSSH, there is no simple solution to this problem, and we will simply renormalize our probability results. In most cases below, the total probability is not far from 1 (<5%).

4. RESULTS

We now present IA-FSSH, F-FSSH, and exact results for the modified Tully model problems presented above.

4.1. Modified Simple Avoided Crossing Problem.

4.1.1. IA-FSSH versus Exact. The transmission probability results for IA-FSSH are shown in Figure 2a,b. The exact results increase smoothly as momentum gets larger in both ω cases (ω = 0.008 and 0.012). IA-FSSH accurately predicts the results for high momentum, where reflection, energy conservation, and velocity rescaling should not be important. However, for low momentum, the results from IA-FSSH deviate from the exact results.

To test whether the energy absorption/emission is correctly predicted, we calculated the final average momentum. As shown in Figure 2g,h, the exact results show a kink at P_0 = 9. This kink comes from the fact that as the initial momentum increases, the wavepacket has just enough energy to move along diabat $|0\rangle$. This effect cannot be recovered by IA-FSSH, which predicts that the transmitted momentum increases steadily as the initial momentum grows.

Next, as shown in Figure 3, according to exact dynamics, the time-dependent model problem yields a new reflection channel through diabatic state $|1\rangle$, in comparison to the original, time-independent model. Unfortunately, IA-FSSH can barely predict such a peak, even though the final momentum can be predicted approximately. Obviously, the performance of IA-FSSH is mixed with respect to modified Tully model problem #1.

4.1.2. F-FSSH versus Exact. Let us now discuss the performance of F-FSSH. The two possible approximations (eqs 44 and 46) for the two ω cases are shown in Figure 2c–f. The first approximation (eq 44), labeled as "F-FSSH pop", accurately predicts the results at the lower momentum regime but cannot predict the oscillations at the high momentum regime, as shown in Figure 2c,d. The second approximation (eq 46), labeled as "F-FSSH inter", as shown in Figure 2e,f, can predict the exact transmission probabilities for all regimes. With regard to the final momentum, note that, unlike IA-FSSH, F-FSSH does recover the correct kink in Figure 2g,h.

As for the new reflection channel, as shown in Figure 3c–f, F-FSSH can recover some reflection approximately in the case of ω = 0.012, but not in the case of ω = 0.008. In the case of ω = 0.008, the reflected final average momentum can barely be predicted by F-FSSH, but the results are predicted qualitatively in the case of ω = 0.012.

4.2. Modified Dual Avoided Crossing Problem.

4.2.1. IA-FSSH versus Exact. For the second modified Tully model problem, as shown in Figure 4a,b, in the case of ω = 0.02, the exact results oscillate strongly while, in the case of ω = 0.04, the exact results are almost flat. Here, we find an interesting nuance: for large frequencies of incoming light, many features of the potential energy surface become washed away and flat scattering probabilities arise. That being said, IA-FSSH can predict the exact results only in the high momentum regime; however, in the low momentum regime, IA-FSSH can only approximately predict the transmission probability. As far as the final average momentum is concerned, IA-FSSH again cannot predict the kink as shown in Figure 4g,h. As far as the reflection channel on diabatic state $|1\rangle$ is concerned, IA-FSSH can hardly predict the peak from the exact results, as shown in Figures 5a,b. From our perspective,

https://dx.doi.org/10.1021/acs.jctc.9b00950
J. Chem. Theory Comput. XXXX, XXX, XXX−XXX

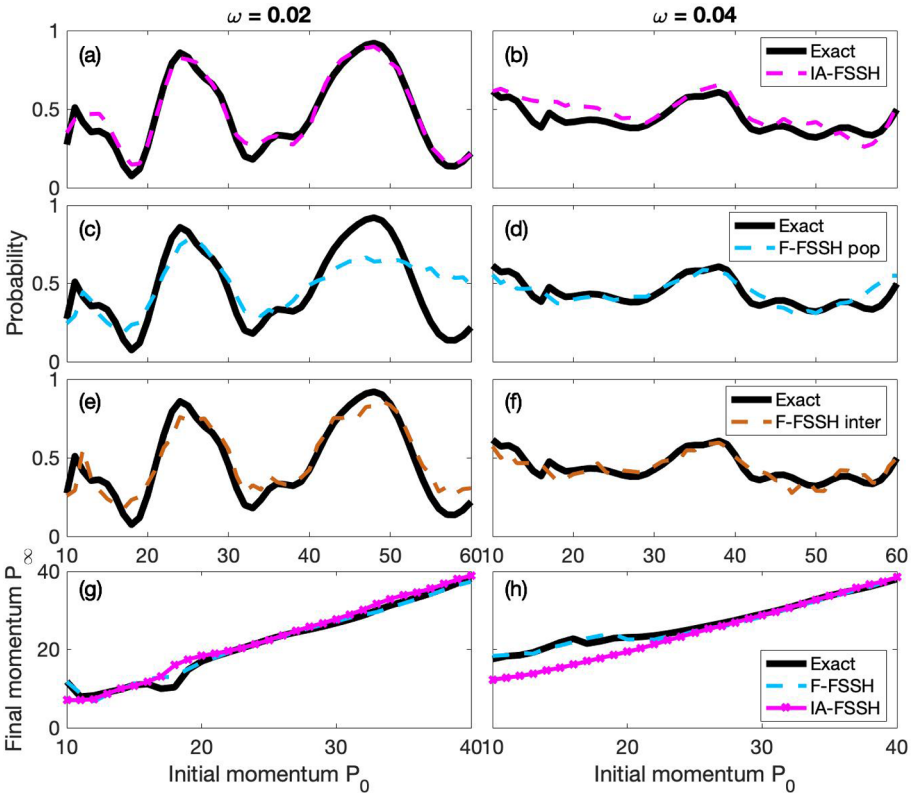

Figure 4. Transmission probabilities and final momenta on diabat $|1\rangle$ for the modified dual avoided crossing problem. The four panels a, c, e, and g on the left show the transmission probabilities and final momentum results for $\omega = 0.02$, and the panels b, d, f, and h on the right side show the results for $\omega = 0.04$. For small ω, IA-FSSH performs extremely well as far as electronic populations are concerned, especially for large momenta. For larger ω, IA-FSSH performs much less well, especially for small momenta. Overall, F-FSSH is roughly as accurate for electronic populations as IA-FSSH, but only using the interference term in eq 46. Moreover, as far as the final momentum is concerned, again only F-FSSH can recover the correct kinks; see panels g and h. The fact that IA-FSSH can recover reasonable electronic populations at large velocities but the accuracy deteriorates at low velocities highlights both the benefits and limitations of not imposing energy conservation/rescaling. Overall, F-FSSH is clearly more reliable.

the fact that IA-FSSH can recover reasonable electronic populations at large velocities—but the accuracy deteriorates at low velocities—highlights both the benefits and limitations of not imposing energy conservation/rescaling. Although not shown, we note that if we do rescale IA-FSSH velocities so as to impose energy conservation artificially, the electronic scattering populations look far worse.

4.2.2. F-FSSH versus Exact. Even though multiple crossings are possible, F-FSSH is again arguably more accurate than IA-FSSH for this model problem. While the first approximation (eq 44) is less accurate than IA-FSSH, the second approximation (eq 46) yields results that are just about as good as IA-FSSH with regard to transmission probability. Moreover, in Figure 4g,h, the final average momentum and the kinks as predicted by F-FSSH are in close agreement with the exact results. Finally, for the reflection channel, as shown in Figure 5c–f, the F-FSSH formalism gives a pretty good estimate of the reflection probabilities (and the final average momenta are qualitatively correct)—unlike IA-FSSH.

Obviously, by reducing a time-dependent problem to a time-independent nonadiabatic problem, where standard FSSH applies and energy conservation can be enforced, F-FSSH becomes far more accurate than IA-FSSH.

5. DISCUSSION: CONVERGENCE TO TIME-INDEPENDENT SIMPLE AVOIDED CROSSING RESULTS

While the results above strongly suggests that F-FSSH is promising (especially in the reasonably low momentum regime) for modeling nonadiabatic dynamics under illumination, one key point that has not yet been addressed is the $\omega \to 0$ limit.[63] As the frequency ω in eq 47 and eq 48 approaches zero, all of our modified model Hamiltonians become the original, time-independent Tully model Hamiltonians and one must wonder: Will F-FSSH reduce to standard FSSH (as IA-FSSH is guaranteed to do)? The answer is not clear because although Floquet states will approach one another, they will always remain separate, each with their own individual dynamics. In this limit, there will be many Floquet states involved and the role of interference term is likely to grow. Does F-FSSH agree with FSSH here?

To test this limit, we have run simulations. As shown in Figure 6a, at high momentum ($P_0 > 10$), where there are only two transmission channels, the F-FSSH algorithm does reduce to time-independent results if we include the interference term. At low momentum, however, the interference term becomes highly oscillatory and F-FSSH no longer matches FSSH. As also shown in Figure 6b, the interference term is unstable and F-FSSH cannot predict the reflection probability on the reflection channel along $|0\rangle$. Notably, renormalizing all

https://dx.doi.org/10.1021/acs.jctc.9b00950
J. Chem. Theory Comput. XXXX, XXX, XXX−XXX

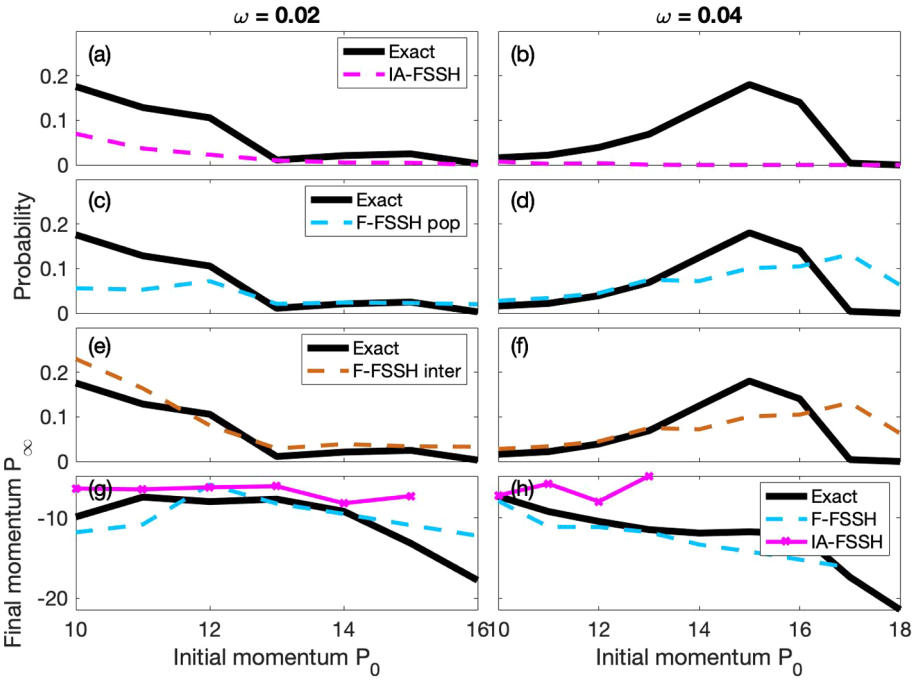

Figure 5. Reflection probabilities on diabat $|1\rangle$ for modified dual avoided crossing problem. All figures represent the same quantities as Figure 4 except now we plot the reflection channel. IA-FSSH predicts a very small reflection probability along this new channel, while F-FSSH formalism recovers the correct trend.

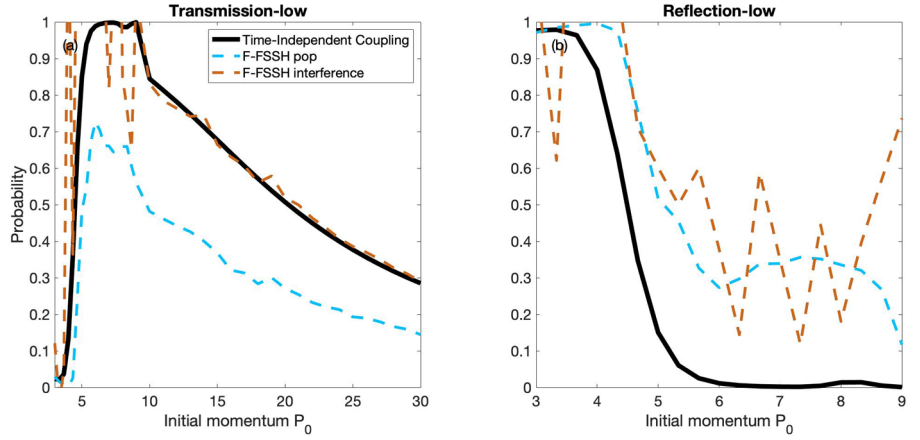

Figure 6. Comparison between time-independent coupling simple avoided crossing model results and the F-FSSH results with $\omega = 0.00001$. Both the transmission (a) and reflection (b) probabilities at lower channels are shown above. The black line represents results for the time-independent Tully's simple avoided model problem. F-FSSH results for $\omega = 0.00001$ show convergence to the time-independent results occurs only in the high momentum regime when including the interference term. Note that, for this figure (as opposed to all other figures in this work), we have not renormalized the total transmission probabilities; see section 3.9. In the low momentum regime, the interference term is highly oscillatory and cannot converge to the time-independent results.

populations to add up to 1 can now (apparently) make things worse. As mentioned above, the coherence problem is not simple, since we must evaluate the coherence between Floquet states generated from the same electronic state and along which the forces are exactly the same, so that previous work on decoherence with surface hopping is not obviously relevant.[19−35] A new understanding of coherence and decoherence in the content of F-FSSH will be necessary, and it would appear fruitful at this time to turn to the QCLE guidance,[18,56] or perhaps exact factorization.[64−67]

In the meantime, how are we to run F-FSSH dynamics if ω changes and goes from finite to zero? In Schmidt et al.'s original F-FSSH work,[41] when dealing with light pulse, the authors switched between standard, adiabatic Born−Oppenheimer states and adiabatic Floquet states for time intervals without or with light pulses. In this slightly modified version of the F-FSSH formalism, there was no additional cost for switching back and forth between algorithms since one can always change the couplings in the Floquet Hamiltonian when the light pulse approaches. For now, if ω ever vanishes, we believe this combination of F-FSSH and FSSH is optimal. In particular, when $V \leq \hbar\omega$, we suggest running F-FSSH and switching to standard FSSH when $V \gg \hbar\omega$. More generally, however, the question remains about what to do when the instantaneous frequency ω depends on time. For this scenario, our instinct is to follow the prescription in ref 41—whereby

https://dx.doi.org/10.1021/acs.jctc.9b00950
J. Chem. Theory Comput. XXXX, XXX, XXX−XXX

hops can occur based on $\frac{d\omega}{dt}$ (just like normal FSSH allows for hops proportional to $\frac{dR}{dt}$, where R is some nuclear coordinate). Alternatively, if we have a situation with two or more frequencies, we can simply use a many-mode Floquet expansion.[68]

6. CONCLUSIONS

In conclusion, we have compared two surface hopping formalisms for extending FSSH into time-dependent regimes. For our model problems, neither transmission probabilities nor reflection probabilities can be completely recovered by IA-FSSH; this formalism can yield nearly exact results at high momentum regime, but less accurate results are predicted by IA-FSSH in the low momentum regime. While we believe this failure cannot be resolved within the current implementation of IA-FSSH, it would be interesting to reexamine these results using a QCLE-based surface hopping method.[69] By contrast, F-FSSH appears to be reasonably accurate for both low and high momenta (though sometimes not quite as good as IA-FSSH for electronic populations at very large high momenta).

With regard to nuclear observables, F-FSSH can yield a good estimate of the resulting momentum in each channel of reflection and transmission, as compared to the exact results. The kink in the middle momentum regime in Figure 2g,h and Figure 4g,h represents the situation in which the transmission channel along diabat $|0\rangle$ is dressed with 0 photon (see Figure 1a, the top red state) and the channel along diabatic state $|1\rangle$ dressed with 2 photons (see Figure 1a, the top blue state) start to participate, and this transmission can be recovered by F-FSSH while the IA-FSSH washes out this effect. Obviously, the ability to impose energy conservation is a big plus for F-FSSH over IA-FSSH when it comes to nuclear observables or other results in the low energy regime. We remind the reader that, in the present contribution, we have not rescaled any IA-FSSH velocities so that there is no notion of any form of energy conservation in the present IA-FSSH results; although not shown, including velocity rescaling appears to make IA-FSSH worse. Future work on the instantaneous adiabatic approach will no doubt need to worry about this problem of energy conservation, e.g., it may well lead to a breakdown of detailed balance.[70,71]

As far as the model problem studied in this work (eqs 47 and 48), we must note that our results for the time-dependent versions of Tully's model problem do depend on where the trajectories start $R(t = 0)$. In Figures 2−5, we initialized all trajectories to start at $R = -9.0$ at time 0. Obviously, because the diabatic coupling is time-dependent, the outcome of a scattering event will depend critically on when a trajectory reaches the effective coupling region or, equivalently, the initial phase of the time-dependent diabatic coupling. In eqs 47 and 48, we choose $\cos(\omega t)$ at the initial position so as to obtain a real Floquet Hamiltonian, yet different results will be obtained with different phases for the diabatic coupling, e.g., $\cos(\omega t + \zeta)$. Such results will be presented and discussed in the following paper in this issue.[60] For real life experiments, unless one can lock in a relationship between the initial phase of the diabatic coupling and the initial position of an initial wavepacket, one would need to average over all initial phases ζ (or several initial positions), and presumably, the averaged results would be identical to the blue dashed line labeled as F-FSSH pop. Thus, the question of whether or not we can observe the oscillations in transmission (as predicted in Figures 2−5) remains open.

Lastly concerning the case $\omega \to 0$, F-FSSH cannot always guarantee reliable electronic amplitudes $\tilde{c}_{n\mu}$ for calculating the interference term in eq 46, as shown in the $\omega = 0.00001$ case, especially when the intensity of the coupling is strong or the frequency is low enough to get more Floquet states involved. We conclude that the regime in which F-FSSH breaks down is when both the coupling strength V and the kinetic energy of the nuclei T are much greater than the energy $\hbar\omega$ of the light. In such a case, for now, we believe the prescription of ref 41 is good enough: run F-FSSH when $V \leq \hbar\omega$ and switch to standard FSSH when $V \gg \hbar\omega$.

In the end, F-FSSH clearly has promise for propagating dynamics with time-dependent couplings. The algorithm is stable, efficient, and easily incorporated to deal with complicated problems involving light−matter interaction, especially at reasonably low intensity. In our calculations, the cost of F-FSSH is roughly six times the cost of IA-FSSH. Furthermore, we believe many improvements are possible in the future, with regard to coherence and decoherence. Assuming the algorithm can be extended easily and accurately to the case of non-CW external fields (as in ref 41), we expect F-FSSH to be the focus of much attention in the years to come.

AUTHOR INFORMATION

Corresponding Author

Joseph Eli Subotnik − *University of Pennsylvania, Philadelphia, Pennsylvania*; Email: subotnik@sas.upenn.edu

Other Authors

Zeyu Zhou − *University of Pennsylvania, Philadelphia, Pennsylvania*; orcid.org/0000-0001-8681-9460

Hsing-Ta Chen − *University of Pennsylvania, Philadelphia, Pennsylvania*; orcid.org/0000-0002-6619-1861

Abraham Nitzan − *University of Pennsylvania, Philadelphia, Pennsylvania*; orcid.org/0000-0002-8431-0967

Complete contact information is available at: https://pubs.acs.org/10.1021/acs.jctc.9b00950

Notes

The authors declare no competing financial interest.

ACKNOWLEDGMENTS

This work was supported by the U.S. Air Force Office of Scientific Research (USAFOSR) AFOSR Grant Nos. FA9550-18-1-0497 and FA9550-18-1-0420. J.E.S. and A.N. thank Eli Pollak for very interesting conversations about Floquet theory.

REFERENCES

(1) Regan, P. M.; Langford, S. R.; Orr-Ewing, A. J.; Ashfold, M. N. The ultraviolet photodissociation dynamics of hydrogen bromide. *J. Chem. Phys.* **1999**, *110*, 281−288.

(2) Franks, K. J.; Li, H.; Kong, W. Orientation of pyrimidine in the gas phase using a strong electric field: Spectroscopy and relaxation dynamics. *J. Chem. Phys.* **1999**, *110*, 11779−11788.

https://dx.doi.org/10.1021/acs.jctc.9b00950
J. Chem. Theory Comput. XXXX, XXX, XXX−XXX

(3) Corrales, M.; González-Vázquez, J.; Balerdi, G.; Solá, I.; De Nalda, R.; Bañares, L. Control of ultrafast molecular photodissociation by laser-field-induced potentials. *Nat. Chem.* **2014**, *6*, 785.
(4) Hilsabeck, K. I.; Meiser, J. L.; Sneha, M.; Harrison, J. A.; Zare, R. N. Nonresonant photons catalyze photodissociation of phenol. *J. Am. Chem. Soc.* **2019**, *141*, 1067−1073.
(5) Hilsabeck, K. I.; Meiser, J. L.; Sneha, M.; Balakrishnan, N.; Zare, R. N. Photon catalysis of deuterium iodide photodissociation. *Phys. Chem. Chem. Phys.* **2019**, *21*, 14195−14204.
(6) Glownia, J.; Natan, A.; Cryan, J.; Hartsock, R.; Kozina, M.; Minitti, M.; Nelson, S.; Robinson, J.; Sato, T.; van Driel, T.; et al. Self-referenced coherent diffraction x-ray movie of ångstrom-and femtosecond-scale atomic motion. *Phys. Rev. Lett.* **2016**, *117*, 153003.
(7) Fuller, F. D.; Gul, S.; Chatterjee, R.; Burgie, E. S.; Young, I. D.; Lebrette, H.; Srinivas, V.; Brewster, A. S.; Michels-Clark, T.; Clinger, J. A.; et al. Drop-on-demand sample delivery for studying biocatalysts in action at X-ray free-electron lasers. *Nat. Methods* **2017**, *14*, 443.
(8) Marquetand, P.; Nogueira, J.; Mai, S.; Plasser, F.; González, L. Challenges in simulating light-induced processes in DNA. *Molecules* **2017**, *22*, 49.
(9) Bajo, J. J.; González-Vázquez, J.; Sola, I. R.; Santamaria, J.; Richter, M.; Marquetand, P.; González, L. Mixed quantum-classical dynamics in the adiabatic representation to simulate molecules driven by strong laser pulses. *J. Phys. Chem. A* **2012**, *116*, 2800−2807.
(10) Tully, J. C. Molecular dynamics with electronic transitions. *J. Chem. Phys.* **1990**, *93*, 1061−1071.
(11) Richter, M.; Marquetand, P.; González-Vázquez, J.; Sola, I.; González, L. SHARC: ab initio molecular dynamics with surface hopping in the adiabatic representation including arbitrary couplings. *J. Chem. Theory Comput.* **2011**, *7*, 1253−1258.
(12) Mai, S.; Marquetand, P.; González, L. Nonadiabatic dynamics: The SHARC approach. *Wiley Interdiscip. Rev.: Comput. Mol. Sci.* **2018**, *8*, e1370.
(13) Mitrić, R.; Petersen, J.; Wohlgemuth, M.; Werner, U.; Bonačić-Koutecký, V. Field-induced surface hopping method for probing transition state nonadiabatic dynamics of Ag 3. *Phys. Chem. Chem. Phys.* **2011**, *13*, 8690−8696.
(14) Lisinetskaya, P. G.; Mitrić, R. Simulation of laser-induced coupled electron-nuclear dynamics and time-resolved harmonic spectra in complex systems. *Phys. Rev. A: At., Mol., Opt. Phys.* **2011**, *83*, 033408.
(15) Thachuk, M.; Ivanov, M. Y.; Wardlaw, D. M. A semiclassical approach to intense-field above-threshold dissociation in the long wavelength limit. *J. Chem. Phys.* **1996**, *105*, 4094−4104.
(16) Thachuk, M.; Ivanov, M. Y.; Wardlaw, D. M. A semiclassical approach to intense-field above-threshold dissociation in the long wavelength limit. II. Conservation principles and coherence in surface hopping. *J. Chem. Phys.* **1998**, *109*, 5747−5760.
(17) Mitrić, R.; Petersen, J.; Bonačić-Koutecký, V. Laser-field-induced surface-hopping method for the simulation and control of ultrafast photodynamics. *Phys. Rev. A: At., Mol., Opt. Phys.* **2009**, *79*, 053416.
(18) Horenko, I.; Schmidt, B.; Schütte, C. A theoretical model for molecules interacting with intense laser pulses: The Floquet-based quantum-classical Liouville equation. *J. Chem. Phys.* **2001**, *115*, 5733−5743.
(19) Schwartz, B. J.; Rossky, P. J. Aqueous solvation dynamics with a quantum mechanical solute: computer simulation studies of the photoexcited hydrated electron. *J. Chem. Phys.* **1994**, *101*, 6902−6916.
(20) Bittner, E. R.; Rossky, P. J. Quantum decoherence in mixed quantum-classical systems: Nonadiabatic processes. *J. Chem. Phys.* **1995**, *103*, 8130−8143.
(21) Schwartz, B. J.; Bittner, E. R.; Prezhdo, O. V.; Rossky, P. J. Quantum decoherence and the isotope effect in condensed phase nonadiabatic molecular dynamics simulations. *J. Chem. Phys.* **1996**, *104*, 5942−5955.
(22) Prezhdo, O. V.; Rossky, P. J. Evaluation of quantum transition rates from quantum-classical molecular dynamics simulations. *J. Chem. Phys.* **1997**, *107*, 5863−5878.
(23) Prezhdo, O. V.; Rossky, P. J. Mean-field molecular dynamics with surface hopping. *J. Chem. Phys.* **1997**, *107*, 825−834.
(24) Fang, J.-Y.; Hammes-Schiffer, S. Improvement of the internal consistency in trajectory surface hopping. *J. Phys. Chem. A* **1999**, *103*, 9399−9407.
(25) Fang, J.-Y.; Hammes-Schiffer, S. Comparison of surface hopping and mean field approaches for model proton transfer reactions. *J. Chem. Phys.* **1999**, *110*, 11166−11175.
(26) Volobuev, Y. L.; Hack, M. D.; Topaler, M. S.; Truhlar, D. G. Continuous surface switching: An improved time-dependent self-consistent-field method for nonadiabatic dynamics. *J. Chem. Phys.* **2000**, *112*, 9716−9726.
(27) Hack, M. D.; Truhlar, D. G. Electronically nonadiabatic trajectories: Continuous surface switching II. *J. Chem. Phys.* **2001**, *114*, 2894−2902.
(28) Wong, K. F.; Rossky, P. J. Dissipative mixed quantum-classical simulation of the aqueous solvated electron system. *J. Chem. Phys.* **2002**, *116*, 8418−8428.
(29) Wong, K. F.; Rossky, P. J. Solvent-induced electronic decoherence: Configuration dependent dissipative evolution for solvated electron systems. *J. Chem. Phys.* **2002**, *116*, 8429−8438.
(30) Horenko, I.; Salzmann, C.; Schmidt, B.; Schütte, C. Quantum-classical Liouville approach to molecular dynamics: Surface hopping Gaussian phase-space packets. *J. Chem. Phys.* **2002**, *117*, 11075−11088.
(31) Jasper, A. W.; Truhlar, D. G. Electronic decoherence time for non-Born-Oppenheimer trajectories. *J. Chem. Phys.* **2005**, *123*, 064103.
(32) Bedard-Hearn, M. J.; Larsen, R. E.; Schwartz, B. J. Mean-field dynamics with stochastic decoherence (MF-SD): A new algorithm for nonadiabatic mixed quantum/classical molecular-dynamics simulations with nuclear-induced decoherence. *J. Chem. Phys.* **2005**, *123*, 234106.
(33) Subotnik, J. E.; Shenvi, N. Decoherence and surface hopping: When can averaging over initial conditions help capture the effects of wave packet separation? *J. Chem. Phys.* **2011**, *134*, 244114.
(34) Subotnik, J. E.; Shenvi, N. A new approach to decoherence and momentum rescaling in the surface hopping algorithm. *J. Chem. Phys.* **2011**, *134*, 024105.
(35) Landry, B. R.; Subotnik, J. E. How to recover Marcus theory with fewest switches surface hopping: Add just a touch of decoherence. *J. Chem. Phys.* **2012**, *137*, 22A513.
(36) Mignolet, B.; Curchod, B. F. Excited-State Molecular Dynamics Triggered by Light Pulses−Ab Initio Multiple Spawning vs Trajectory Surface Hopping. *J. Phys. Chem. A* **2019**, *123*, 3582−3591.
(37) Petit, A. S.; Subotnik, J. E. How to calculate linear absorption spectra with lifetime broadening using fewest switches surface hopping trajectories: A simple generalization of ground-state Kubo theory. *J. Chem. Phys.* **2014**, *141*, 014107.
(38) Petit, A. S.; Subotnik, J. E. Calculating time-resolved differential absorbance spectra for ultrafast pump-probe experiments with surface hopping trajectories. *J. Chem. Phys.* **2014**, *141*, 154108.
(39) Miao, G.; Subotnik, J. E. Revisiting the Recoherence Problem in the Fewest Switches Surface Hopping Algorithm. *J. Phys. Chem. A* **2019**, *123*, 5428−5435.
(40) Martens, C. C. Surface hopping by consensus. *J. Phys. Chem. Lett.* **2016**, *7*, 2610−2615.
(41) Fiedlschuster, T.; Handt, J.; Schmidt, R. Floquet surface hopping: Laser-driven dissociation and ionization dynamics of H 2+. *Phys. Rev. A: At., Mol., Opt. Phys.* **2016**, *93*, 053409.
(42) Hammes-Schiffer, S.; Tully, J. C. Proton transfer in solution: Molecular dynamics with quantum transitions. *J. Chem. Phys.* **1994**, *101*, 4657−4667.
(43) Fabiano, E.; Keal, T.; Thiel, W. Implementation of surface hopping molecular dynamics using semiempirical methods. *Chem. Phys.* **2008**, *349*, 334−347.

https://dx.doi.org/10.1021/acs.jctc.9b00950
J. Chem. Theory Comput. XXXX, XXX, XXX−XXX

(44) Barbatti, M.; Pittner, J.; Pederzoli, M.; Werner, U.; Mitrić, R.; Bonačić-Koutecký, V.; Lischka, H. Non-adiabatic dynamics of pyrrole: Dependence of deactivation mechanisms on the excitation energy. *Chem. Phys.* **2010**, *375*, 26−34.
(45) Plasser, F.; Granucci, G.; Pittner, J.; Barbatti, M.; Persico, M.; Lischka, H. Surface hopping dynamics using a locally diabatic formalism: Charge transfer in the ethylene dimer cation and excited state dynamics in the 2-pyridone dimer. *J. Chem. Phys.* **2012**, *137*, 22A514.
(46) Fernandez-Alberti, S.; Roitberg, A. E.; Nelson, T.; Tretiak, S. Identification of unavoided crossings in nonadiabatic photoexcited dynamics involving multiple electronic states in polyatomic conjugated molecules. *J. Chem. Phys.* **2012**, *137*, 014512.
(47) Nelson, T.; Fernandez-Alberti, S.; Roitberg, A. E.; Tretiak, S. Artifacts due to trivial unavoided crossings in the modeling of photoinduced energy transfer dynamics in extended conjugated molecules. *Chem. Phys. Lett.* **2013**, *590*, 208−213.
(48) Wang, L.; Prezhdo, O. V. A simple solution to the trivial crossing problem in surface hopping. *J. Phys. Chem. Lett.* **2014**, *5*, 713−719.
(49) Meek, G. A.; Levine, B. G. Evaluation of the time-derivative coupling for accurate electronic state transition probabilities from numerical simulations. *J. Phys. Chem. Lett.* **2014**, *5*, 2351−2356.
(50) Jain, A.; Alguire, E.; Subotnik, J. E. An efficient, augmented surface hopping algorithm that includes decoherence for use in large-scale simulations. *J. Chem. Theory Comput.* **2016**, *12*, 5256−5268.
(51) Dell' Angelo, D.; Hanna, G. Importance of eigenvector sign consistency in computations of expectation values via mixed quantum-classical surface-hopping dynamics. *Theor. Chem. Acc.* **2017**, *136*, 75.
(52) Lee, E. M.; Willard, A. P. Solving the trivial crossing problem while preserving the nodal symmetry of the wavefunction. *J. Chem. Theory Comput.* **2019**, *15*, 4332−4343.
(53) Kosloff, R. Time-dependent quantum-mechanical methods for molecular dynamics. *J. Phys. Chem.* **1988**, *92*, 2087−2100.
(54) Subotnik, J. E.; Jain, A.; Landry, B.; Petit, A.; Ouyang, W.; Bellonzi, N. Understanding the surface hopping view of electronic transitions and decoherence. *Annu. Rev. Phys. Chem.* **2016**, *67*, 387−417.
(55) Donoso, A.; Martens, C. C. Simulation of coherent non-adiabatic dynamics using classical trajectories. *J. Phys. Chem. A* **1998**, *102*, 4291−4300.
(56) Kapral, R.; Ciccotti, G. Mixed quantum-classical dynamics. *J. Chem. Phys.* **1999**, *110*, 8919−8929.
(57) Subotnik, J. E.; Ouyang, W.; Landry, B. R. Can we derive Tully's surface-hopping algorithm from the semiclassical quantum Liouville equation? Almost, but only with decoherence. *J. Chem. Phys.* **2013**, *139*, 214107.
(58) Kapral, R. Surface hopping from the perspective of quantum−classical Liouville dynamics. *Chem. Phys.* **2016**, *481*, 77−83.
(59) Loring, T. A. Computing a logarithm of a unitary matrix with general spectrum. *Numer. Linear Algebr. Appl.* **2014**, *21*, 744−760.
(60) Zhou, Z.; Jin, Z.; Qiu, T.; Rappe, A. M.; Subotnik, J. E. A Robust and Unified Solution for Choosing the Phases of Adiabatic States as a Function of Geometry: Extending Parallel Transport Concepts to the Cases of Trivial and Near-Trivial Crossings. *J. Chem. Theory Comput.* **2019**, DOI: 10.1021/acs.jctc.9b00952.
(61) Jain, A.; Subotnik, J. E. Surface hopping, transition state theory, and decoherence. II. Thermal rate constants and detailed balance. *J. Chem. Phys.* **2015**, *143*, 134107.
(62) Jasper, A. W.; Truhlar, D. G. Improved treatment of momentum at classically forbidden electronic transitions in trajectory surface hopping calculations. *Chem. Phys. Lett.* **2003**, *369*, 60−67.
(63) Hone, D. W.; Ketzmerick, R.; Kohn, W. Time-dependent Floquet theory and absence of an adiabatic limit. *Phys. Rev. A: At., Mol., Opt. Phys.* **1997**, *56*, 4045−4054.
(64) Abedi, A.; Maitra, N. T.; Gross, E. K. Exact factorization of the time-dependent electron-nuclear wave function. *Phys. Rev. Lett.* **2010**, *105*, 123002.
(65) Abedi, A.; Maitra, N. T.; Gross, E. Correlated electron-nuclear dynamics: Exact factorization of the molecular wavefunction. *J. Chem. Phys.* **2012**, *137*, 22A530.
(66) Suzuki, Y.; Abedi, A.; Maitra, N. T.; Gross, E. Laser-induced electron localization in H2+: mixed quantum-classical dynamics based on the exact time-dependent potential energy surface. *Phys. Chem. Chem. Phys.* **2015**, *17*, 29271−29280.
(67) Min, S. K.; Agostini, F.; Tavernelli, I.; Gross, E. K. Ab initio nonadiabatic dynamics with coupled trajectories: A rigorous approach to quantum (de) coherence. *J. Phys. Chem. Lett.* **2017**, *8*, 3048−3055.
(68) Ho, T.-S.; Chu, S.-I.; Tietz, J. V. Semiclassical many-mode Floquet theory. *Chem. Phys. Lett.* **1983**, *96*, 464−471.
(69) Rekik, N.; Hsieh, C.-Y.; Freedman, H.; Hanna, G. A mixed quantum-classical Liouville study of the population dynamics in a model photo-induced condensed phase electron transfer reaction. *J. Chem. Phys.* **2013**, *138*, 144106.
(70) Parandekar, P. V.; Tully, J. C. Mixed quantum-classical equilibrium. *J. Chem. Phys.* **2005**, *122* (9), 094102.
(71) Schmidt, J. R.; Parandekar, P. V.; Tully, J. C. Mixed quantum-classical equilibrium: Surface hopping. *J. Chem. Phys.* **2008**, *129* (4), 044104.

https://dx.doi.org/10.1021/acs.jctc.9b00950
J. Chem. Theory Comput. XXXX, XXX, XXX−XXX